J. A. Viator, S. L. Jacques, S. A. Prahl, "Generating subsurface acoustic waves in indocyanine green stained elastin biomaterial using a Q-switched laser," in *Laser-Tissue Interaction IX*, S. L. Jacques Ed., Proc. SPIE 3254, 104–111, (1998).

Generating subsurface acoustic waves in indocyanine green stained elastin biomaterial using a Q-switched laser

John A. Viator, Steve L. Jacques, Scott A. Prahl

Oregon Graduate Institute, Portland, OR 97291
Oregon Medical Laser Center, Portland, OR 97225

ABSTRACT

A Q-switched frequency-doubled Nd:YAG laser coupled to an optical parametric oscillator generated 4.75 ns 800 nm laser pulses to create a subsurface acoustic wave in planar indocyanine green gel samples and flat segments of elastin biomaterial stained with indocyanine green. The acoustic waves traveled through the target and were detected by a piezoelectric transducer. The waveforms were converted to measurements of pressure (and temperature) as a function of depth in the material. An algorithm was developed and applied to the acoustic signals to extract information about the the absorption coefficient as a function of depth in the samples.

Keywords: photoacoustic imaging, photothermal imaging, depth profiling, absorption coefficient

1. INTRODUCTION AND BACKGROUND

Laser tissue welding is a thermal process in which two tissues are fused together using laser energy. Laser welding is proposed as an alternative to suture techniques, since it is potentially faster and less traumatic.[1] Numerous investigations on tissue welding have been undertaken, including those using indocyanine green (ICG) as a chromophore to localize laser energy deposition at the welding site. Since the welding process depends on temperature, accurate measurement of the thermal profile at the welding site is critical for understanding the mechanism of laser welding. Furthermore, the initial distribution of ICG at the welding site is a crucial parameter in the welding process. In this paper we use a photoacoustic technique[2] to obtain thermal profiles as a function of depth in tissues stained with ICG. We also develop and apply a simple algorithm for extracting information about the absorption coefficient (or ICG concentration) as a function of depth from the acoustic signals.

An acoustically-confined[3] laser pulse will create a pressure wave in an absorbing sample (biomaterial or gelatin, Figure 1). This pressure wave will propagate in both directions along the laser beam axis, each with half of the original amplitude.[2] The acoustic signal, detected at a short distance from the site of the initial pressure wave, contains information about the initial temperature and pressure and consequently about the distribution of dye in the material.

2. MATERIALS AND METHODS

An ICG-dyed gel and ICG-stained elastin biomaterial are used as targets from which acoustic waves are generated and detected. The gel, being homogeneous, has uniform absorption while the elastin biomaterial is expected to have a dye layer that drops in concentration with depth.

2.1. Q-switched Laser

The laser used for these experiments was a Q-switched frequency doubled Nd:YAG laser (Quantel Brilliant) operating at 532 nm coupled to an optical parametric oscillator (OPOTEK) tuned to 800 nm. All laser pulses for these experiments were performed as single shots of 40 mJ. The pulse duration (FWHM) was 4.75 ns. The laser spot was elliptical, with major and minor diameters of 3 and 2 mm, respectively.

Direct correspondence to S.A.P, prahl@ece.ogi.edu; (503) 216–2197; http://omlc.ogi.edu

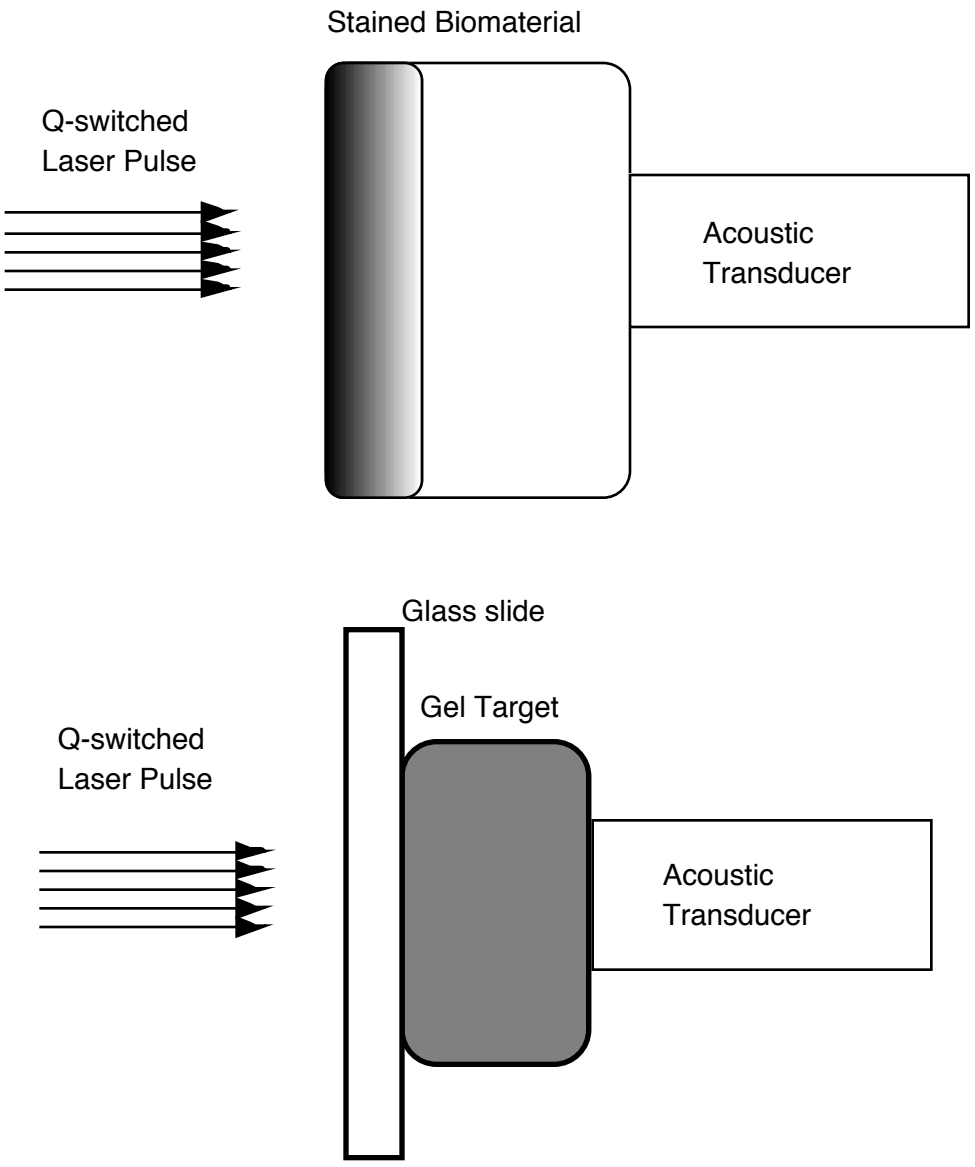

Figure 1. ICG stained elastin biomaterial. The dye layer concentration decreases with depth (top). The ICG dyed gelatin target. The dye concentration is uniform throughout. The gel was set on a glass slide (bottom).

2.2. Indocyanine Green Gel

The absorbing gel was prepared as 3.5% gelatin (175 Bloom) in 15 ml of water with 0.0171 g of indocyanine green dye. This corresponds to a 2 mM concentration, similar to that used in many tissue welding experiments. The absorption coefficient at 800 nm was 190 cm^{-1}. The gel was formed directly on glass slides and allowed to cool so that the glass-gel interface would be free of air bubbles. The glass slide provided support for the thin gelatin sample during irradiation. The thickness of the gel was measured with a micrometer and was approximately 750 μm.

2.3. Elastin Biomaterial

Elastin biomaterial is formed from the elastin constituent of an aorta. In these experiments the elastin biomaterial was derived from porcine aorta harvested from domestic swine. The aorta was cleaned and placed in a 0.5 M sodium hydroxide at 65°C. The vessels were sonicated for 60 minutes. The vessels were then rinsed in deionized water. This process resulted in the removal of all constituents of the artery except for the elastin layer. The thickness of the tissue was measured with a micrometer and was approximately 1 mm. The biomaterial was cut open so that a flat, rectangular piece could be positioned in the path of the laser beam. The intimal surface was stained by brushing a 2 mM ICG dye solution onto the biomaterial. The opposite surface contacted a piezoelectric transducer.

2.4. Piezoelectric Transducer

The piezoelectric transducer (Science Brothers, WAT-12) is a LiNbO crystal used for detecting acoustic pulses of nanosecond duration. The sensing element is protected by a germanium window that is opaque to the 800 nm laser light. The delay in the transducer is 700 ns, determined by placing the stained biomaterial surface directly onto the germanium window, with no intervening stained tissue. The signal was detected after 700 ns, the delay being attributed to the time for the acoustic signal to travel from the site of laser deposition through the germanium window and onto the sensing element.

3. RESULTS

3.1. Gel Response

The signal detected by the acoustic transducer for the absorption in the gel is shown in the top graph of Figure 2. Equivalent temperatures are shown on the right vertical axis. The relation

$$T = \frac{P}{\rho c \Gamma} \tag{1}$$

is used, where P is pressure [J/cm^3], ρ is the density [g/cm^3], c is the specific heat [J/g°C], and Γ is the unitless Grüneisen coefficient. The value $\Gamma = 0.12$ was used in this paper.[2] The relation

$$10\,\text{bar} = 1\,\text{J/cm}^3 \tag{2}$$

should be used to convert pressures in bars to energy density. The total delay after the trigger pulse is shown on the horizontal axis. The less smooth negative pressure (tensile wave) that follows is probably caused by an acoustic diffractive effect of the beam boundaries. The tensile wave is not a reflection at a free surface, since the gel to glass coupling was free from air bubbles. The total delay of the initial stress wave is 1100 ns, so subtracting the transducer delay of 700 ns, gives a propagation time through the gel of 400 ns, indicating a gel thickness of 600 μm. This result assumes a sound propagation speed c_s of 1.5 mm/μs. This is less than the measured thickness of 750 μm, but the transducer placed against the gel surface may have caused some compression, thus reducing the gel thickness.

The bottom graph of Figure 2 is the initial acoustic wave generated in the ICG gel, where the times t from the top graph have been converted to depths z within the gelatin using $z = (1.1\mu\text{s} - t)c_s$. The solid line is an exponential curve fit, given by

$$P(z) = 4.21 \exp(-178\text{cm}^{-1} z) \qquad \text{(bar)} \tag{3}$$

The fit is close for most of the curve, but shows significant disagreement at the surface ($z = 0$). This may be due to diffraction or complications from the glass-gel boundary.

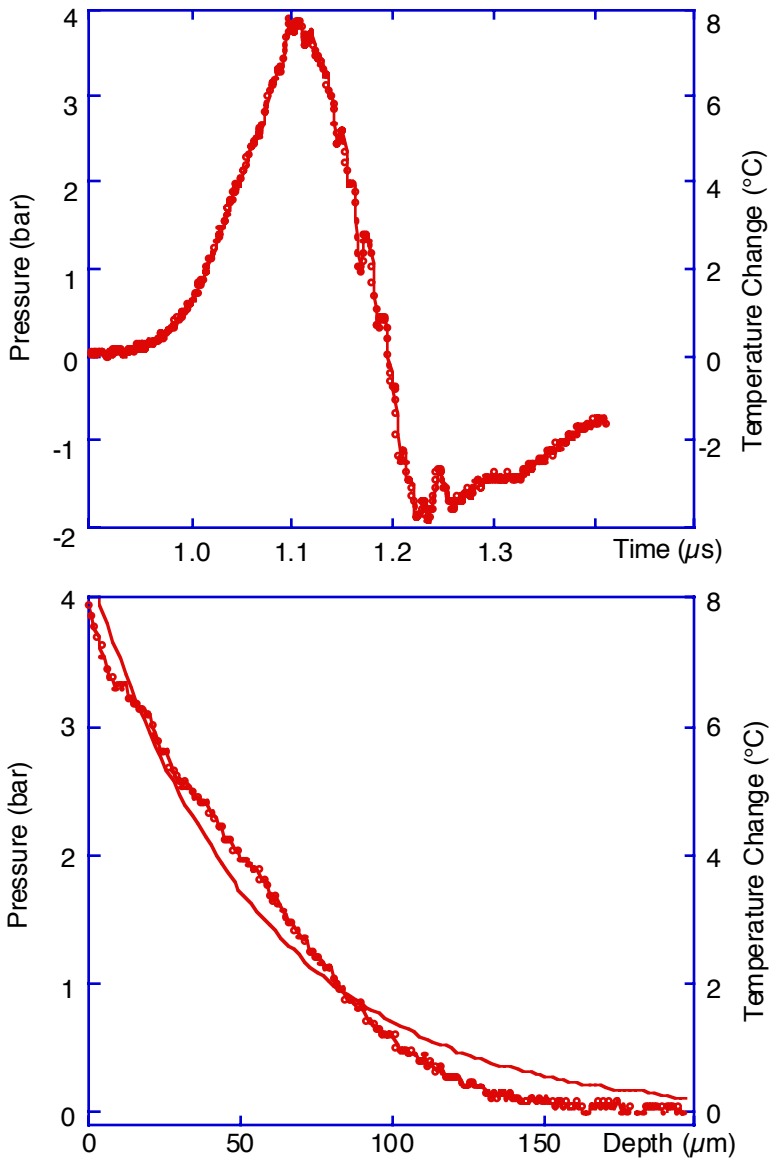

Figure 2. (Top) The acoustic wave from the ICG gel. The time scale is set to zero at the beginning of the Q-switched pulse. (Bottom) The initial acoustic wave generated in the ICG gel, showing pressure as a function of depth. The solid line is an exponential curve fit.

3.2. Elastin Biomaterial Response

The acoustic signal detected from the stained elastin biomaterial is shown in the top graph of Figure 3. In this case, the front of the tissue is bounded by air, thus creating a free surface, which results in a following tensile wave described earlier. This feature is shown here, although the tensile wave is attenuated. The total delay for the initial stress wave after the trigger, 1400 ns, is indicated on the horizontal axis. Since the detector delay is 700 ns, the propagation time through the tissue is 700 ns. This gives a tissue thickness of 1050 μm, which agrees with the measured thickness of 1000 μm.

The bottom graph of Figure 3 shows the initial acoustic wave generated in the stained biomaterial. In this case, the times t from the top graph have been converted to depths z within the biomaterial using $z = (1.42\mu\text{s} - t)c_s$. The right vertical axis directly gives the temperature rise in the elastin biomaterial as a function of depth.

4. DISCUSSION

4.1. Absorption Coefficient of ICG Gel

The absorption coefficient of the ICG gel was selected as 190 cm^{-1} to be comparable to the absorption of a lightly stained ICG biomaterial.[4] This corresponds to an absorption depth of about 50 μm. The elastin biomaterial waveform shows the initial stress which indicates a dye deposition depth of 30 μm (Figure 6).

4.2. Diffraction Effects

The analysis of the stress wave assumes a planar wave front. Diffractive effects become important when the size of the initial stress field is comparable to the distance that the pressure waves must propagate to the acoustic detector. The gelatin stress waves propagated 750 μm and the biomaterial stress waves propagated about 950 μm. Since the initial stress field was only 2000 μm across, diffractive effects will affect the detected signal.

4.3. Frequency Response of the Piezoelectric Transducer

The sensitivity of the piezoelectric transducer is dependent on the frequency of the detected signal. The manufacturer's supplied sensitivity calibration was used to convert the signal amplitude in millivolts to a pressure in bars. In the case of the gel and elastin biomaterial, 20 MHz and 50 MHz were used as signal frequencies, respectively. The calibration curve gave a value of 20 mV/bar and 40 mV/bar, respectively.

Fourier analysis was performed on the signal generated from the gel sample and on the predicted signal pressures from the gel to determine the frequency response of the transducer. Since the gel absorption coefficient was known to be 190 cm^{-1} and assuming a homogeneous distribution of ICG in the gel, the transducer sensitivity as a function of frequency was calculated. The sensitivity was flat except for a decrease by a factor of two at the higher frequencies.

4.4. Derivation of Absorption Coefficient

The pressure and temperature rise following the laser pulse is explicit in Figures 2 and 3, but the variation in ICG concentration is implicit. To calculate the intrinsic absorption as a function of depth, we developed a simple model based on an absorbing-only medium.

For a uniformly absorbing medium exposed to a laser pulse with a radiant exposure of H_0, the energy A_1 absorbed per unit area in a layer with thickness Δx_1 is

$$A_1 = H_0\big(1 - \exp(-\mu_a \Delta x_1)\big) \tag{4}$$

For a two layer medium, the energy absorbed per unit area in the second layer is reduced by the amount lost in passing through the first layer with thickness Δx_1,

$$A_2 = H_0\big(1 - \exp(-\mu_{a2} \Delta x_2)\big) \exp(-\mu_{a1} \Delta x_1) \tag{5}$$

Extending this to a multi-layer case, the energy per unit area absorbed in the n^{th} layer is

$$A_n = H_0\big(1 - \exp(-\mu_{an} \Delta x)\big) \exp\Big(-\sum_{i=1}^{n-1} \mu_{ai} \Delta x\Big) \tag{6}$$

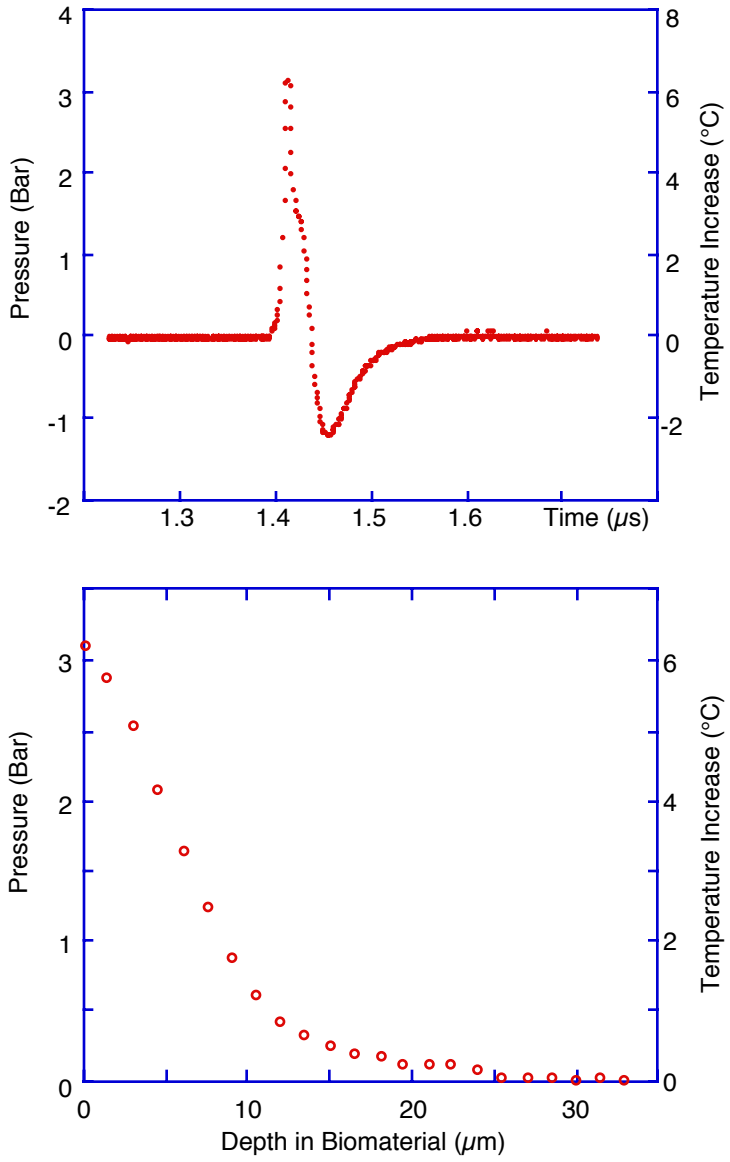

Figure 3. (Top) The acoustic signal from the stained biomaterial. The time scale is set to zero at the beginning of the Q-switched pulse. (Bottom) The initial positive pressure wave as a function of depth derived from the signal at the top. No exponential curve fit was made because the dye concentration is not expected to be uniform.

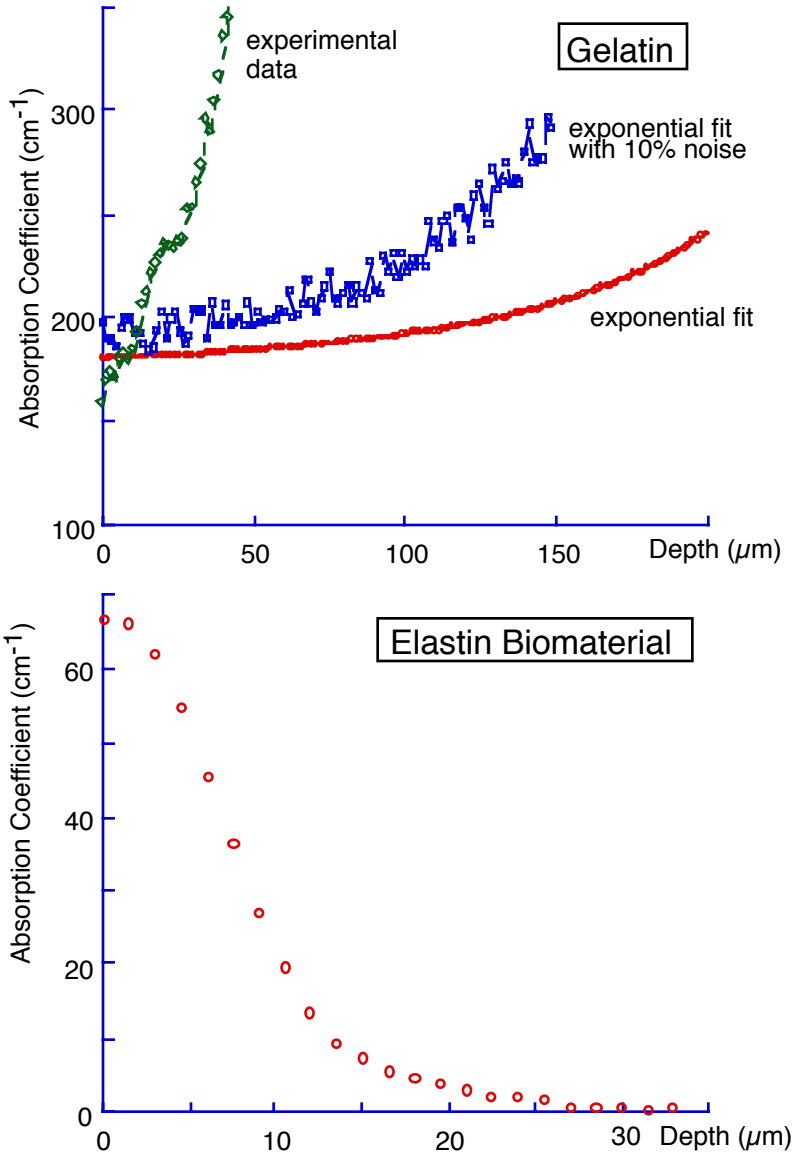

Figure 4. The absorption coefficient calculated using equation (8). The top graph shows the results for data obtained using the exponential fit of equation (3), the exponential fit (3) with 10% noise, and for the experimental data in Figure (2). The bottom graph shows the results for the stained biomaterial.

Since equation (6) is expressed in terms of energy per unit area, the relationship $P_n = \Gamma A_n/\Delta x$ may be used to obtain the pressures that propagate in each direction,

$$P_n = \frac{\Gamma H_0}{2\Delta x}\big(1 - \exp(-\mu_{an}\Delta x)\big)\exp\Big(-\sum_{i=1}^{n-1}\mu_{ai}\Delta x\Big) \tag{7}$$

(The factor of two arises because half the energy propagates in each direction along the axis of the laser beam.) Note, that if the radiant exposure is given in J/cm^2 and the layer thickness is in cm, then equation (7) will generate pressures with units of J/cm^3. To obtain pressures in bars, then equation (2) should be used.

An equation for the absorption coefficient of each layer can be derived from equation (7).

$$\mu_{an} = -\frac{1}{\Delta x}\ln\left(1 - \frac{2\Delta x P_n}{\Gamma H_0}\exp\Big(\sum_{i=1}^{n-1}\mu_{ai}\Delta x\Big)\right) \tag{8}$$

Again, the pressure P should be in J/cm^3, the layer thickness Δx should be in cm, and the radiant exposure H_0 should be in J/cm^2. If the target material is divided into layers corresponding to the resolution of the waveform on the digitizing signal analyzer, the absorption coefficient can be derived for each of these layers using the algorithm described above. The absorption coefficients are obtained with increasing depths, starting with the first layer and propagating downwards into the sample.

To illustrate the stability of the algorithm, noiseless data was generated using equation (3) and processed using equation (8). This is shown in the top graph of Figure 4 for the data labeled "exponential fit." To show the sensitivity of the algorithm to noise, 10% noise was added to the exponential data and the results are also shown in the top graph of Figure 4. Finally, the actual data shown in Figure 2 is processed using equation (8) and shown in the same graph. The absorption coefficients increase with depth, contrary to the known uniform absorption coefficient of the gel.

The algorithm is unstable for the experimental data. While the initial absorption coefficient of 180 cm^{-1} is reasonable, the values diverge almost immediately. The curve fit result, showing an absorption coefficient of about 180 cm^{-1} for the first 150 μm, is much better behaved. Even with the noise added, the curve fit result shows an calculated absorption coefficient of 180–200 cm^{-1} for the first 100 μm. The algorithm is very sensitive to artifacts in the experimental data, while the curve fits are generally faithful to the known absorption. As noted before, the data at the surface of the gel departs from the exponential fit. This may cause an early error in the algorithm computation, though the result would probably only manifest itself as an magnitude, not the extreme divergence shown here. Interestingly, all three curves show an increasing absorption with depth. This indicates a bias in the algorithm to process error in one direction, regardless of the nature of the perturbation in the data.

The bottom graph in Figure 4 shows the calculated absorption coefficient of the ICG stained elastin biomaterial. The exponential decay of the absorption is expected for the staining. The divergence shown in the gel calculations is not evident here, perhaps due to the fact that the staining depth is less than 30 μm, so the algorithm may not have manifested its latent instability.

5. ACKNOWLEDGEMENTS

We would like to acknowledge the help of Gary Gofstein for assistance in the acoustic wave detection experiment. We also acknowledge the help of Dr. Alexander Oraevsky of Rice University for his help on the acoustic transducers. This work was supported by the Department of the Army Combat Casualty Care Division, US AMRMC contract 95221N–02, and by the Department of Energy, DE–FG03–97–ER62346.

REFERENCES

1. L. S. Bass and M. R. Treat, "Laser tissue welding: A comprehensive review of current future clinical applications," *Lasers Surg. Med.* **17**, pp. 315–349, 1996.
2. A. A. Oraevsky, S. L. Jacques, and F. K. Tittel, "Mechanism of laser ablation for aqueous media irradiated under stress confined conditions," *J. Appl. Phys.* **78**, pp. 1281–1289, 1995.

3. S. L. Jacques, "Laser-tissue interactions. Photochemical, photothermal and photomechanical," *Lasers General Surg.* **72**, pp. 531–557, 1992.
4. K. S. Kumar, "Spectroscopy of indocyanine green photodegradation," Master's thesis, Oregon Graduate Institute of Science and Technology, 1996.